Evaluating reporter genes of different luciferases for optimized in vivo bioluminescence imaging of transplanted neural stem cells in the brain

ARTICLE *in* CONTRAST MEDIA & MOLECULAR IMAGING · NOVEMBER 2013

Impact Factor: 2.92 · DOI: 10.1002/cmmi.1549 · Source: PubMed

CONTRAST MEDIA & MOLECULAR IMAGING

Received: 29 January 2013, Revised: 7 May 2013, Accepted: 10 May 2013, Published online in Wiley Online Library

(wileyonlinelibrary.com) DOI: 10.1002/cmmi.1549

Evaluating reporter genes of different luciferases for optimized *in vivo* bioluminescence imaging of transplanted neural stem cells in the brain

Laura Mezzanotte[a†], Markus Aswendt[b†], Annette Tennstaedt[b], Rob Hoeben[c], Mathias Hoehn[b] and Clemens Löwik[a*]

Bioluminescence imaging (BLI) has become the method of choice for optical tracking of cells in small laboratory animals. However, the use of luciferases from different species, depending on different substrates and emitting at distinct wavelengths, has not been optimized for sensitive neuroimaging. In order to identify the most suitable luciferase, this quantitative study compared the luciferases Luc2, CBG99, PpyRE9 and hRluc. Human embryonic kidney (HEK-293) cells and mouse neural stem cells were transduced by lentiviral vector-mediated transfer to express one of the four luciferases, together with copGFP. A T2A peptide linker promoted stoichiometric expression between both imaging reporters and the comparison of cell populations upon flow cytometry. Cell dilution series were used to determine highest BLI sensitivity *in vitro* for Luc2. However, Coelenterazine h-dependent hRluc signals clearly exceeded D-luciferin-dependent BLI *in vitro*. For the quantitative *in vivo* analysis, cells were transplanted into mouse brain and BLI was performed including the recording of emission kinetics and spectral characteristics. Differences in light kinetics were observed for D-luciferin vs Coelenterazine h. The emission spectra of Luc2 and PpyRE9 remained almost unchanged, while the emission spectrum of CBG99 became biphasic. Most importantly, photon emission decreased in the order of Luc2, CBG99, PpyRE9 to hRluc. The feasibility of combining different luciferases for dual color and dual substrate neuroimaging was tested and discussed. This investigation provides the first complete quantitative comparison of different luciferases expressed by neural stem cells. It results in a clear recommendation of Luc2 as the best luciferase selection for *in vivo* neuroimaging.

Supporting information may be found in the online version of this paper

Keywords: luciferase; kinetics; emission spectrum; noninvasive; multicolor; neuroimaging; neural stem cells; transplantation

1. INTRODUCTION

Bioluminescence imaging (BLI) has been widely used in the last decade to visualize *in vivo* molecular events and has been successfully applied in preclinical studies of tumor development (1), stem cell tracking (2), visualization of microbial infections (3) and immunological responses (4). BLI meets the requirements of a simple and cost-effective molecular imaging technique with superior sensitivity in superficial and deep tissue measurements (5–7). This optical technique allows the monitoring of different molecular events simultaneously thanks to the use of luciferase enzymes that are dependent on specific substrates or emit at different wavelengths (8–10). Nevertheless, the ideal luciferase/substrate combination has to be determined for each application to achieve optimal sensitivity. In particular, three luciferase/substrate groups are available for *in vivo* imaging in mammalian cells: (a) ATP-dependent firefly and click beetle luciferases that use D-luciferin as a substrate (5,11,12); (b) ATP-independent luciferases from *Gaussia princeps* (13,14) and *Renilla* (15), which require Coelenterazine as a substrate, and luciferases from *Cypridina noctiluca* and *Vargula hilgendorfii* that utilize vargulin as a substrate (16); and (c) bacterial luciferases which were genetically modified to generate their substrate autonomously (17,18). Table 1 summarizes the corresponding luciferase characteristics. Despite the gain in knowledge about wild-type and mutant luciferases for *in vivo* imaging applications, conditions for optimized bioluminescence neuroimaging have not been systematically investigated yet. Optical methods to visualize neural stem cells *in vivo* mainly

* *Correspondence to: C. Löwik, Experimental Molecular Imaging, Department of Radiology, Leiden University Medical Center, Leiden, The Netherlands. Email: c.w.g.m.lowik@lumc.nl*

† *The first two authors contributed equally to this work.*

a *L. Mezzanotte, C. Löwik*
Experimental Molecular Imaging, Department of Radiology, Leiden University Medical Center, Leiden, The Netherlands

b *M. Aswendt, A. Tennstaedt, M. Hoehn*
In-vivo-NMR Laboratory, Max Planck Institute for Neurological Research, Cologne, Germany

c *R. Hoeben*
Department of Molecular Cell Biology, Leiden University Medical Center, Leiden, The Netherlands

Table 1. Properties of luciferases from different species

Luciferase	Species	Peak emission *in vitro*	Peak emission *in vivo*	Quantum yield	Substrate used	Protein size	Energy source	Requirements	Reference
Luc2	*Photinus pyralis*	557 nm[c]	610 nm	0.41	D-Luciferin	61 kDa	ATP[a]	O_2, Mg^{2+}	(41,46)
PpyRE9	*Photinus pyralis*	617 nm[c]	617 nm	N.A.	D-Luciferin	61 kDa	ATP	O_2, Mg^{2+}	(11)
CBG99	*Pyrophorus plagiophthalamus*	537 nm[d]	537 nm	0.62	D-Luciferin	64 kDa	ATP	O_2	(12,41)
GLuc	*Gaussia princeps*	485 nm	N.A	N.A.	Coelentera-zine	19 kDa	Substrate	O_2	(13)
hRluc	*Renilla reniformis*	480 nm[d]	480 nm	0.06	Coelentera-zine	34 kDa	Substrate	O_2	(15,41)
Cluc	*Cypridina noctiluca*	465 nm[e]	N.A.	0.3	Vargulin	62 kDa	Substrate	O_2	(16)
Lux ABCDE	*Vibrio Harvey*	490 nm	N.A.	0.16	Aldehyde and $FMNH2^b$	77 kDa (LuxA,B)	Substrate	O2,	(17)

[a]Adenosine triphosphate; [b]flavin mononucleotide; [c]purified enzyme at 25°C, pH 7.8; [d]cell lysate at 25°C pH 7.8; [e]enzyme at 25°C pH 7.4.

rely on the expression of reporter genes inserted by lentiviral vector-mediated gene transfer. Pseudoviral particles can be used to infect neural cells *in vivo* by stereotactical injection (19,20), or by *in vitro* transduction of neural (stem) cell lines (21,22).

For neuroimaging application, we validated and compared state-of-the-art luciferases, including the codon-optimized firefly luciferase Luc2, the red codon-optimized mutant PpyRE9, the codon-optimized Renilla luciferase h-Rluc and the green click beetle luciferase CBG99. Human embryonic kidney cells (HEK-293) and murine neural stem cells (NSCs) were transduced to express the luciferases under control of a strong constitutive EF1 promoter. All cells were sorted by fluorescence activated cell sorting (FACS) for equimolar expression of a T2A-coupled copGFP reporter (23). Experiments included validation of the BLI signal from cells *in vitro* and *in vivo* after intracerebral transplantation. This study was intended to provide essential imaging reporter characterization and selection for optical stem cell tracking in the mouse brain.

2. EXPERIMENTAL

2.1. Cell Culture

Human embryonic kidney cells (HEK-293) were routinely cultured in DMEM (Invitrogen, Darmstadt, Germany) supplemented with 10% FCS (Invitrogen), 1% penicillin–streptomycin (PAA, Pashing, Austria) and 2 mM L-glutamine (PAA).

The generation of radial glia-like NSCs from the murine embryonic stem (ES) cell line D3 was achieved by adaptation of previously described protocols (24,25). The ES cell line D3 (26) (generous gift of Dr Tomo Saric, Institute of Neurophysiology, University Cologne, Germany) was cultured on mitotically inactivated mouse fibroblast cells as previously described (27). Embryoid body (EB) formation was induced in suspension for 4 days in DMEM supplemented with 15% FCS (Invitrogen), 1× nonessential aminoacids (PAA), 2 mM L-glutamine (PAA). EBs were converted into neurosphere-like aggregates by culturing in N2/B27 medium consisting of DMEM/F12, Neurobasal, 1× B27, 1× N2 (all from Invitrogen) and 2 mM L-glutamine, changing the medium every 3–4 days. After 10–14 days, the neurosphere-like EBs were cultured on flasks coated with 0.2% gelatin (Sigma-Aldrich, Schnelldorf, Germany). Twenty-four hours later, the medium was changed to N2Euro medium consisting of Euromed-N (Biozol, Eiching, Germany), 10 ng/ml EGF (Epidermal Growth Factor) (Preprotech, Hamburg, Germany), 10 ng/ml b-FGF (Basic Fibroblast Growth Factor) (Peprotech), 50 μg/ml bovine serum albumin (PAA), 25 μg/ml insulin (Sigma-Aldrich) and 1× N2. The N2Euro medium promoted proliferation of EGF and b-FGF responsive stem cells, while non-NSCs were removed by culturing for 20 days until the final NSC line (D3WT_N2Euro) was established. D3WT_N2Euro cells exhibit a radial glia-like NSC phenotype, express a set of corresponding radial glia ($BLBP^+$/$GFAP^-$) and NSC markers ($Nestin^+$/$Pax6^+$/$Sox1^-$/$Sox2^+$/$Musashi1^+$/$Prominin\text{-}1^+$) and differentiate into neurons and glia (28). All cells were cultured under humidified 5% CO_2 and 95% air.

2.2. Cloning of Luciferases into Lentiviral Plasmids

Each luciferase was cloned into the multiple cloning site (MCS) of the lentiviral expression vector pCDH-EF1-MCS-T2A-copGFP (System Biosciences, Mountain View, CA, USA) using specific

primers with the corresponding restriction sites. Expression in the lentiviral plasmid is driven by the housekeeping elongation factor 1α (EF1) promoter. The superbright green fluorescent protein copGFP (30) from the copepod *Pontenilla plumata* (excitation/emission maximum = 482/502 nm) was used for normalization of transgene expression. The vector allows bicistronic expression of a recombinant DNA and the copGFP via the 'self-cleaving' T2A peptide. The luciferase Luc2 was amplified from pGL4.14 (Promega, Madison, WI, USA) using the following pair of primers: Luc2-**BamHI**-for 5′-AAGGGAAA**GGATCC**GCCACCATGGAAGATGCC AAAA ACATTAAG-3′and Luc2-rev-**NotI** 5′-AAATTT**GCGGCCGC**CA CGGCGATCTTGC-3′. The luciferase mutant PpyRE9 was amplified from pGEX-PpyRE9 (generous gift of Professor B Branchini, Connecticut College, New London, CT, USA) using the following pair of primers: PpyRE9-**BamHI**-for 5′-AAGGAAAAA**GGATCC**GCC ACCATGGAGGACGCCAAG-3′ and PpyRE9-rev-**NotI** 5′-AAATTT**GCG GCCGC**GATCTTGCCGCCC-3′. The click beetle luciferase CBG99 was amplified from pGL3 (Promega) using the following pair of primers: CBG99-**BamHI**-for 5′-AAGGGAAAA**GGATCC**GCCACCATG GTGAAGCGT GAG-3′ and CBG99-**NotI**-rev 5′-TAAAA**GCGGCCGC** ACCGCCGGC-3′. The codon-optimized Renilla luciferase hRluc was amplified from pGL4.7 (Promega) using the following pair of primers: hRluc-**XbaI**-for 5′-AAGGGAAAATCTAGAGCCACCATGG CTTCCAAG-3′ and hRluc-**NotI**-rev 5′-TAAAAGCCGGATCCCTGCTC GTTCTTCAG-3′. All plasmids were verified by sequencing.

2.3. Lentiviral Production and Transduction of Cells

The lentiviruses were produced as described previously (29). Virus was quantified by antigen capture ELISA measuring HIV p24 levels (ZeptoMetrix Corporation, NY, USA). This value was converted to an infectious titer using the approximation that 1 ng of p24 equals 2500 infectious units. HEK-293 and NSCs were transduced by pseudoviral particles using 40 ng virus per 1×10^5 cells.

2.4. Flow Cytometry

Stable clones were isolated by cell sorting using a FACSAriaII (Becton Dickinson, Franklin Lakes, NJ, USA) on the basis of their copGFP expression. GFP fluorescence was detected using a 530/30 nm band-pass filter (FL1 channel) following excitation with an argon ion laser source at 488 nm. Using a forward-scatter/side-scatter representation of events, a region to exclude cellular debris from the analysis and a region to collect highly positive cells were defined. A number of events/FL1 (which reflects the fluorescence intensity) histogram was established and used to select GFP-positive cells. Different gates were used for NSCs and HEK 293 cells populations. For each 10 000 events were collected.

2.5. *In vitro* Imaging

Luciferase-expressing cells were plated in different amounts (1000, 2500, 5000 and 10 000 NSCs and 5, 50, 100, 250, 500 and 1000 HEK-293 cells) in black 96-well plates (nunc™, Rochester, NY, USA) and 100 µl phosphate buffered saline. All images were taken with the IVIS® Spectrum imaging system (Caliper Life Sciences, Hopkinton, MA, USA) using an open filter and a series of band pass filters for 1 s at 5 min after addition of 0.2 mM D-luciferin (Synchem, Felsberg, Germany) or directly after addition of 60 µM of XenoLight RediJect Coelenterazine h (Caliper Life Sciences). For checking equimolar expression of copGFP, 10^4 cells for each sorted population were plated and fluorescence measurements (excitation filter 475 nm and emission filter 520 nm, 2 s acquisition) were performed before addition of D-luciferin or Coelenterazine h. For comparison with *in vivo* BLI, all *in vitro* measurements were performed at 37°C. Analysis was performed using the Living Image software version 4.0 (Caliper Life Sciences). Light output from specified circular regions of interest (0.02 cm^2) was quantified as photon flux (p/s) while image pixel threshold was set a 1.14×10^3 pixels per second. For fluorescence measurement light output from the same region of interest was quantified as radiation efficiency $(p/s/cm^2/sr)/(\mu W/cm^2)$.

2.6. Cell Transplantations

Animal experiments were reviewed and approved by the Bioethics Committee of the Leiden University, The Netherlands. All animals received humane care in compliance with the 'Code of Practice Use of Laboratory animals in Cancer Research' (Inspectie W&V, July 1999). For surgery and imaging sessions, 8-week-old female mice (Balb/c Nu/Nu or Balb/c, Charles River Laboratories, Wilmington, DE, USA; $n = 18$) were anesthetized with isoflurane in O_2:N_2O (30:70%). Intracerebral transplantations were performed by fixing the mouse in a stereotactic frame (Stoelting Dublin, Ireland). The skull was exposed by a small incision and one or two holes were drilled at the following coordinates relative to bregma: AP +0.5; L ±2.0; DV −4.0/−3.0/−1.5. The homogeneous cell suspensions were kept on ice during the surgery and were subsequently injected into the brain through a Hamilton syringe (23G needle). Different cell amounts were injected in a volume of 2 µl.

2.7. *In vivo* Imaging

The *in vivo* set-up included an open filter measurement for 30 s with a binning of 8 × 8 pixels, f/stop 1 and 4 cm field of view. Luciferase kinetics were recorded by consecutive 30 s acquisitions for 30 min upon D-luciferin (150 mk/kg) or Coelenterazine h (1.5 mg/kg) injection at 24 h post-transplantation of 3×10^5 HEK-293 cells into the mouse striatum at 3 mm depth ($n = 3$ per luciferase type). The same mice were used for spectral acquisition 15 min (hRluc) and 20 min (Luc2, CBG99, PpyRE9) after i.p. substrate injection using an exposure time of 30 s for every 20 nm band pass filter (12 filter, total acquisition time ~7 min). For hRluc BLI, additional experiments on three nude mice were carried out at 0.5 and 24 h and 7 days post-transplantation of 1×10^5 into the left and 3×10^5 HEK-293 cells into the right striatum. Consecutive 30 s images were acquired for 25 min upon i.p. or i.v. injection of Coelenterazine h (1.5 mg/kg). *In vivo* photon emission of the four different luciferases expressed by NSCs was compared 24 h post-transplantation of 1×10^5 cells into the left and 3×10^5 cells into the right striatum of nude mice ($n = 3$ for each luciferase, in total $n = 12$). Images were acquired 20 min after i.p. injection of D-luciferin (150 mg/kg) or Coelenterazine h (1.5 mg/kg).

2.8. Dual Reporter Imaging

For evaluation of dual-reporter imaging, the hRluc/Luc2 and CBG99/PpyRE9 luciferase pairs were used. Nude mice ($n = 3$) received a 50:50 mixture of HEK-293 cells expressing hRluc or Luc2 as cell grafts at 3 mm depth into the right striatum. BLI was performed 24 h later by injection of 1.5 mg/kg Coelenterazine h (acquisition started 15 min post-injection), followed by injection of 150 mg/kg D-luciferin (acquisition started 20 min post-injection) with a time delay of 3 h. A control measurement was used to prove the lack of remaining

photon emission from the first imaging session. Proof-of-concept dual color imaging was performed on nude mice ($n = 2$). Then 1.5×10^5 HEK-293 CBG99 cells were transplanted into the right striatum and 1.5×10^5 HEK-293 PpyRE9 cells into the left striatum. In addition, a separate animal received a striatal cell graft of 50:50 mixed 1.5×10^5 CBG99/PpyRE9 expressing HEK-293 cells. Spectral acquisition was performed 20 min after i.p. injection of D-luciferin (150 mg/kg) using an exposure time of 30 s for every 20 nm band pass filter (12 filters, total acquisition time ~7 min).

2.9. Statistics

One-way ANOVA followed by Tukey's test was used to compare the light output from cells expressing the different reporters for *in vitro* and *in vivo* experiments.

3. RESULTS

3.1. Luciferase- and Cell Type-Specific Differences for *in vitro* Bioluminescence

The purpose of this study was to compare the photon emission of recently developed bioluminescence reporter genes (Luc2, CBG99, PpyRE9 and hRluc) for optical neuroimaging. Therefore, we generated self-inactivating, bicistronic lentiviral vectors in which the strong constitutive promoter EF1 drives the expression of one of the 4 luciferases combined with the copGFP sequence via the 'self-cleaving' T2A linker element (Fig. 1a). This approach enabled equimolar expression of two imaging reporters. The human cell line HEK-293 and mouse NSCs (D3WT_N2Euro) – derived from the ES cell line D3WT – were transduced by lentiviral-mediated transfer. For each transduction, 40 ng virus per 10^5 cells were used, which resulted in a transduction efficiency of 80% (HEK-293) and 30% (NSCs). In total, four different cell lines were generated for each cell type, expressing one of the four different luciferases. Cell clones were subsequently sorted in order to enrich the population of cells with a high and homogenous copGFP expression. Different fluorescence gates were necessary for NSCs (2×10^3 to 1×10^4 copGFP counts) and HEK-293 cells (9×10^3 to 2×10^5 copGFP counts). After sorting, equal copGFP expression was validated for each cell type by fluorescence microscopy and fluorescence imaging (Fig. 1b, c). The average fluorescence radiant efficiency was $9.45 \pm 0.13 \times 10^8$ for HEK-293 and $4.26 \pm 0.18 \times 10^8$ for NSCs (Fig. 1c). The luciferase-specific cell detection limit was determined by plating NSCs (Fig. 2a) and HEK-293 cells (Supporting Information, Fig. S1) in a cell dilution series and using bioluminescence imaging with open filter in the presence of D-luciferin (0.2 mM) or Coelenterazine h (60 μM). Based on the quantitative photon flux analysis for each luciferase expressed by either the NSCs (Fig. 2b) or HEK-293 cells (Supporting Information, Fig. S1b), the linear correlation between cell number and photon flux was determined 5 min post-substrate addition (mean $R^2 = 0.99$ for all cell lines). According to the differences in copGFP expression between cell types, there was also a substantial and statistically significant difference in bioluminescence light output (data compared for 1×10^3 cells, Fig. 2c). HEK-293 cells exhibited 4- to 5-fold higher signal intensity than NSCs and were used in the following *in vivo* experiments as a positive control. However, the luciferase photon emission was cell type-independent: Luc2 and CBG99 were brighter than PpyRE9 with differences in light output becoming more significant with increasing cell amounts. NSCs expressing Luc2 exhibited a 1.4 ± 0.1 higher BLI signal compared with CBG99. In relation to PpyRE9, photon fluxes from Luc2 cells were 4.5 ± 0.2 fold higher. The *in vitro* bioluminescence of the Coelenterazine h-dependent hRluc outranged the other luciferases and resulted in a 1.9 ± 0.4-fold higher BLI signal than Luc2.

3.2. *In vivo* Bioluminescence Kinetics, Emission Spectra and Sensitivity

In a first step of *in vivo* luciferase characterization, the kinetics of light emission was recorded. The bioluminescence from 3×10^5 HEK-293 cells at 3 mm depth in the mouse striatum ($n = 3$) was acquired by five or six consecutive measurements for 30 s over a time period of 30 min. All D-luciferin-dependent luciferases exhibited an increasing photon emission until reaching a plateau phase ~20–25 min post D-luciferin injection. In contrast, hRluc bioluminescence peaked already ~12 min post-Coelenterazine

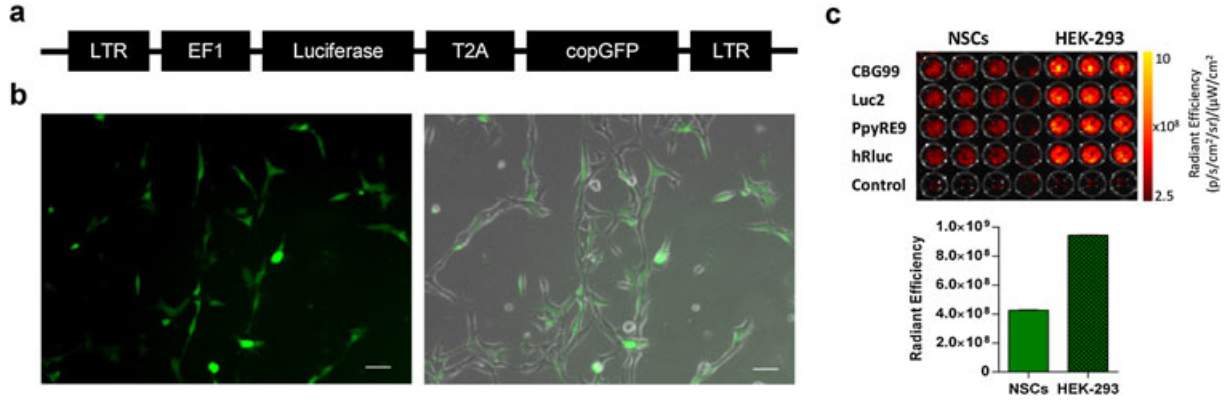

Figure 1. Reporter gene expression in two different cell types. (a) Schematic drawing of a part of the lentiviral plasmid composed of the EF1 promoter driving expression of the luciferase (Luc2, CBG99, PpyRE9, or hRluc) and the fluorescence protein copGFP coupled via a T2A-like sequence. (b) Representative microscopic fluorescence image and the brightfield overlay of neural stem cells (NSCs) after transduction and FACS (20× magnification, scale bar 50 μm). (c) Quantitative fluorescence measurement of 1×10^4 HEK-293 cells and NSCs transduced with lentiviruses for the expression of the different luciferases revealed differences in transgene activity between both cell types. Average fluorescence (samples analyzed in triplicate) for transduced HEK-293 was $9.45 \pm 0.13 \times 10^8$ (p/s/cm^2/sr)/(μW/cm^2) and that for transduced NSCs was $4.26 \pm 0.18 \times 10^8$ (p/s/cm^2/sr)/(μW/cm^2).

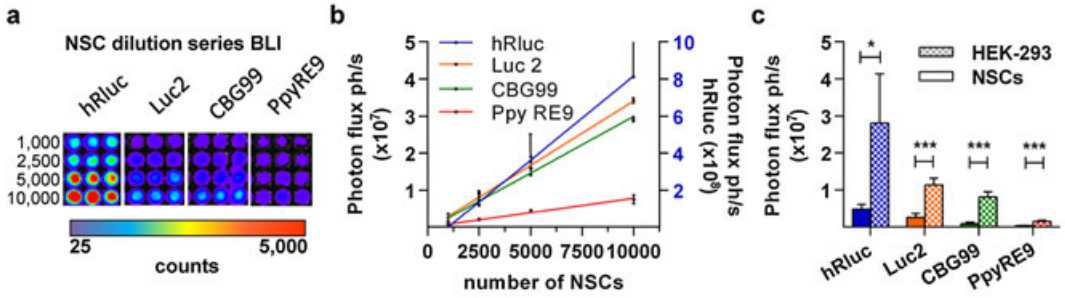

Figure 2. Evaluation of luciferase sensitivity for NSCs *in vitro*. (a) Representative bioluminescence/photography overlay of a NSC dilution series ranging from 1000 to 10 000 cells expressing hRluc, Luc2, CBG99 or PpyRE9. (b) Quantitative analysis of the photon flux in relation to the cell number revealed a linear correlation for every tested luciferase. NSCs expressing hRluc exhibited the highest photon flux (right *y*-axis) followed by the D-luciferin-dependent Luc2, CBG99 and PpyRE9 (left *y*-axis). (c) The luciferase-dependent photon flux differences were cell type independent, as shown by the *in vitro* photon flux comparison between HEK-293 cells and NSCs according to the type of luciferase (experiments in triplicate). HEK-293 cells exhibited significantly higher photon emission for every luciferase referring to a higher gene expression level (level of significance indicated by * $p \leq 0.01$ and *** $p \leq 0.0001$).

h administration (Fig. 3a). Photon emission from Luc2 cells was significantly higher compared with CBG99 (1.6 ± 0.2; $p \leq 0.05$), compared with PpyRE9 (4.4 ± 0.3; $p \leq 0.01$) and also compared with hRluc (50.0 ± 8; $p \leq 0.01$).

In a second step, the same animals were used to record luciferase-specific *in vivo* emission spectra by applying a series of 20 nm band pass filters ranging from 520 to 680 nm. In comparison to the *in vitro* standard, the non-normalized emission spectra of hRluc, Luc2 and PpyRE9 remained almost unchanged at 3 mm depth, while the emission spectrum of CBG99 became biphasic (Fig. 3b). There was no variation between emission spectra obtained at different time points after substrate administration (representative data for PpyRE9 and CBG99 shown in Supporting Information, Fig. S2). In additional experiments, the emission spectrum of CBG99 was further explored: 3×10^5 HEK-293 cells were transplanted at 1.5, 3.0 and 4.0 mm depth (Supporting Information, Fig. S3). The spectral analysis revealed a strong shift of the emission maximum as a function of the transplantation depth with the most prominent difference induced between 1.5 and 3.0 mm.

3.3. Quantitative Luciferase Comparison for Stem Cell Tracking

In order to identify the detection limits and best luciferase for NSC imaging, a separate *in vivo* experiment was performed: NSCs expressing one of the four different luciferases were transplanted at 3 mm depth into the striatum of nude mice (for each luciferase $n = 3$). As shown in Fig. 4a, 3×10^5 (right striatum) and 1×10^5 cells (left striatum) were both visible in the case of Luc2 and CBG99, while only 3×10^5 cells were visible in the case of PpyRE9 (24 h post-transplantation). Quantification of light emission confirmed the differences found *in vitro*. Luc2 signals were significantly higher than CBG99 (1.5 ± 0.2; $p \leq 0.05$) and PpyRE9 (3.7 ± 0.3; $p \leq 0.01$); 1×10^5 PpyRE9 and 1-3×10^5 hRluc cells were not detectable (Fig. 4b).

3.4. Validation of Dual Reporter Neuroimaging

In order to explore the possibility of separating the signal from two different luciferases in one mouse, two settings were used: (a) the substrate-specific luciferase pair Luc2 and hRluc for *dual-substrate imaging*; and (b) the green CBG99 and red PpyRE9 luciferase with distinct emission maxima for *dual color imaging*. In a first set of experiments, we characterized the hRluc *in vivo* characteristics for brain imaging by engrafting 3×10^5 and 1×10^5 HEK-293 cells into the right and left mouse striatum, respectively ($n = 3$). Longitudinal BLI was performed 0.5 and 24 h and 7 days post-transplantation by injection of Coelenterazine h (0.75 mg/kg) and 25 min of BLI (Supporting Information, Fig. S4a). The 1×10^5 cells were only detectable at the first time point. However, 3×10^5 hRluc remained detectable up to 7 days. The BLI signal decreased during the first 24 h by an order of magnitude compared with the 0.5 h time point (Supporting Information, Fig. S4b). Analysis at 0.5 and 24 h and 7 days revealed significant

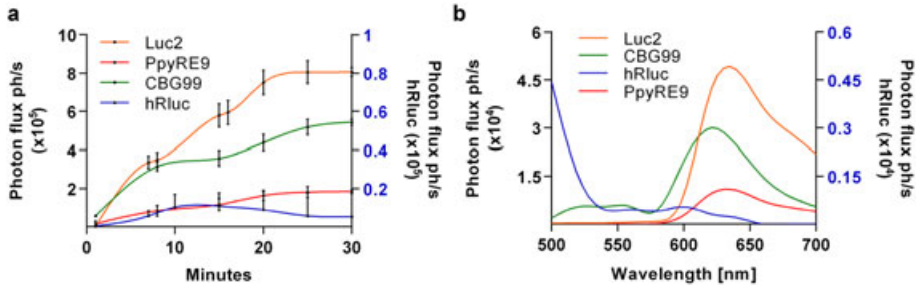

Figure 3. Luciferase-dependent photon flux time curves and emission spectra *in vivo*. (a) Luciferase kinetics were recorded by consecutive 30 s acquisitions for 30 min upon D-luciferin or Coelenterazine h injection at 24 h post-transplantation of 3×10^5 HEK-293 cells. Steady-state photon emission was reached at ~12 min (hRluc) and 20–25 min (D-luciferin-dependent luciferases) after substrate injection. (b) Photon flux plotted against the emission wavelength representing luciferase-specific spectra for the cell graft at 3 mm depth 24 h post-transplantation, recorded 15 min (hRluc) and 20 min (Luc2, CBG99, PpyRE9) post-substrate injection.

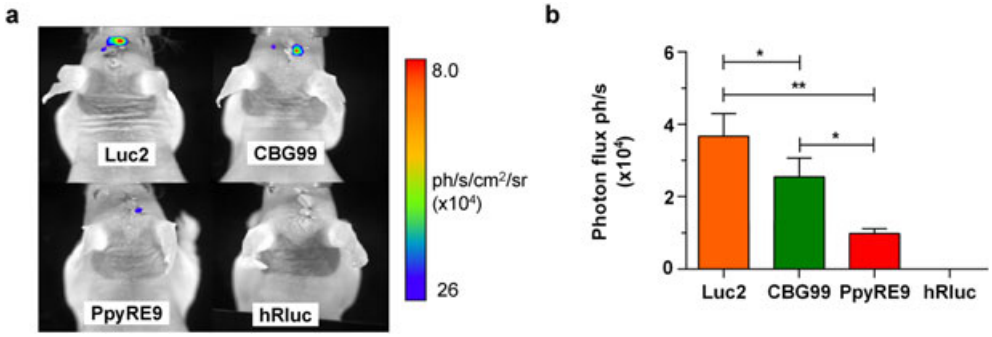

Figure 4. Comparison of Luc2, CBG99, PpyRE9 and hRluc for detection of NSC grafts in the mouse brain. (a) Representative bioluminescence images of 1×10^5 (left striatum) and 3×10^5 (right striatum) Luc2, CBG99, PpyRE9 or hRluc emitting NSCs ($n = 3$). Images were acquired 20 min after D-luciferin and 15 min after Coelenterazine h injection and displayed with equal scale for visual comparison. (b) Photon flux comparison (3×10^5 NSCs) showing the significantly higher photon emission of Luc2 compared with CBG99 (* $p \leq 0.05$) and PpyRE9 (** $p \leq 0.01$).

differences in photon emission (One-way ANOVA $p \leq 0.001$; Tukey's test $p < 0.01$ between 0.5 h and both 24 h and 7 days). The influence of the injection route (i.p. vs i.v.) on the hRluc signal kinetics was compared in three mice at 24 h post-transplantation (Supporting Information, Fig. S4c). Upon i.v. injection the signal decreased rapidly without reaching a long steady-state phase, which limits the reproducibility of repetitive *in vivo* experiments. In contrast, the BLI signal increased with time and reached a plateau phase ~12 min after i.p. injection. Based on these hRluc sensitivity measurements, the combination with Luc2 cells was evaluated: a mixture of 1×10^5 hRluc and 1×10^5 Luc2 expressing HEK-293 cells was transplanted into the right striatum of nude mice ($n = 3$) and imaged 24 h post-transplantation (Fig. 5a). The two different substrates, Coelenterazine h and D-luciferin, were used in two consecutive imaging sessions with a time delay of 3 h – to allow complete disappearance of the hRluc signal. According to the quantitative analysis (Fig. 5b), the Luc2 signal was significantly higher than the hRluc bioluminescence.

In the second set of experiments, we explored the feasibility of dual color imaging in the mouse brain. For this purpose, 1.5×10^5 HEK-293 cells expressing either CBG99 or PpyRE9 were transplanted into the right and left striatum of one nude mouse. In addition, a 50:50 mixture of 1.5×10^5 CBG99 and PpyRE9 HEK-293 cells was transplanted into the right striatum of a separate nude mouse. Both mice were measured 24 h later for bioluminescence simultaneously (Fig. 6a). CBG99 and PpyRE9 signals were discriminated by applying a spectral unmixing algorithm as previously reported (8). However, the accuracy of unmixing was affected by the effective emission spectra (Fig. 6b). The biphasic nature of the CBG99 spectrum including the increased red light component led to an overlap with the red spectrum of the PpyRE9 luciferase. As a result, the unmixing of the bioluminescence signals from the 50/50 mixture of CBG99 and PpyRE9 was achieved only qualitatively.

4. DISCUSSION

4.1. Luciferase- and Cell-Specific Differences for in vitro Bioluminescence

Under *in vitro* conditions, the BLI sensitivity increased from PpyRE9, over CBG99 to Luc2 and hRluc, which is in accordance with previous reports (22,30). Based on the homogeneous detector for the full-range spectrum of visible light, this order is strictly related to the luciferase-specific photon emission quantity per substrate molecule. The imaging protocol was adapted to the different light kinetics in order to exclude effects on the measured photon emission: Renilla luciferases exhibit a flash kinetic with a peak signal in the first 10 s and a fast decline over ~10 min (31) and were measured directly upon substrate administration. In contrast, D-Luciferin-dependent luciferases reach a steady-state photon emission several minutes after substrate administration with a half-life of up to 2 h (32) and were measured 5 min after substrate administration. In conclusion, already at the

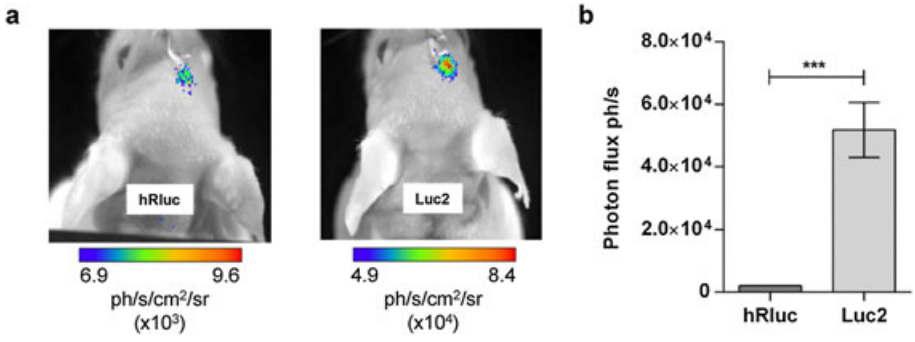

Figure 5. Dual reporter imaging using Luc2 and hRluc expressing HEK-293 cells. (a) A mixture of 1.5×10^5 Luc2 and 1.5×10^5 hRluc expressing HEK-293 cells was transplanted to the right striatum of nude mice ($n = 3$). Representative bioluminescence image at 24 h post-transplantation upon injection of Coelenterazine h followed by injection of D-luciferin with a time delay of 3 h into the same mouse. (b) Quantitative analysis of photon emission from Luc2 and hRluc mixture cell grafts in nude mice ($n = 3$), showing significantly higher BLI signal for Luc2 separated from the hRluc signal by the injection of either D-luciferin or Coelenterazine h (level of significance, *** $p \leq 0.0001$).

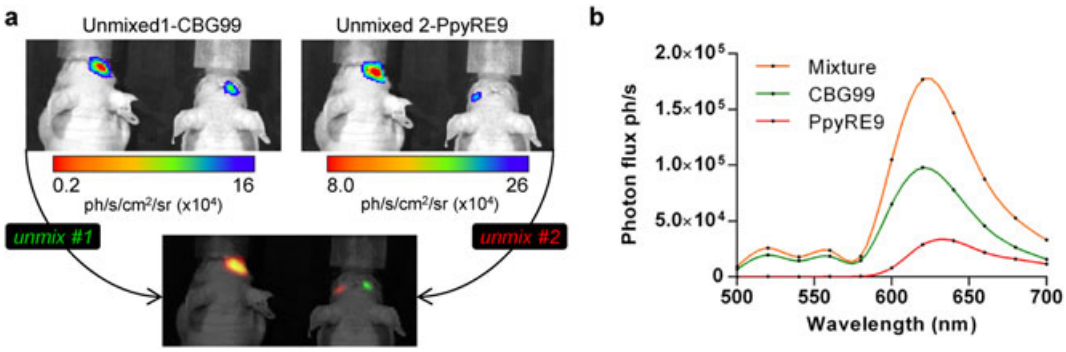

Figure 6. Dual reporter bioluminescence imaging using spectral unmixing algorithm. (a) 1.5×10^5 CBG99 cells were transplanted into the right striatum, 1.5×10^5 PpyRE9 cells into the left striatum of the nude mouse on the right in the picture. In addition, a mixture of both HEK-293 cell lines was transplanted into the right striatum of the separate nude mouse on the left side of the picture. Spectral measurements were performed 24 h later using a series of 20 nm band pass filters (500–700 nm). A spectral unmixing algorithm was applied in order to select green light from CBG99 and red light from PpyRE9. The result of the unmixing on the CBG99/PpyRE9 graft is visualized in orange. (b) Non-normalized emission spectra of CBG99 (green), PpyRE9 cells (red) and the cell mixture (orange) at 3 mm intracerebral transplantation depth.

in vitro level, a direct comparison between both luciferases can only be achieved by adaption of the imaging protocol. Nevertheless, owing to the flash kinetic of hRluc, the maximal photon emission during the short *in vitro* measurement is much higher compared with firefly and click beetle luciferases.

The *in vitro* photon emission of the luciferases was not different for HEK-293 and D3WT_N2Euro. However, the reporter gene expression differed substantially between these two cell types. The robust HEK-293 cells could be transduced with higher efficiency and sorted for high expressing clones with a substantially higher FACS gate compared with the NSCs. The lower efficiency of gene delivery and suppression of exogenous genes integrated into the (embryonic) stem cell genome has been described (33,34). Lentiviral transduction remains the most efficient method for gene transfer into neural progenitor cells (35) without detrimental effects on stem cell differentiation (36). However, potential side effects of imaging reporter overexpression cannot be excluded, as Puttonen *et al*. reported recently (37). The vulnerability of NSCs towards high reporter gene expression limited the imaging reporter expression levels. In contrast, HEK-293 cells are known to resist transgene effects and maintain viability and proliferation (38). The results presented here indicate that the BLI sensitivity *in vitro* depends on the cell type-specific transduction efficiency, transgene integration and transgene expression level.

4.2. *In vivo* Bioluminescence Kinetics and Emission Spectra – Impact on Sensitivity

For the *in vivo* comparison, we selected the model of intracerebrally transplanted cells, which complements to previous reports in different tissue compartments (22,39–41). The order of D-luciferin-dependent luciferase signals was not changed compared with the *in vitro* condition and was also independent of the cell type. Recently, Gil *et al.* (30) compared multiple luciferases by normalization of *in vivo* data using quantitative real-time PCR and concluded that Luc2 is the brightest luciferase for liver imaging, which is in good accordance with our experiments in the mouse brain. The quantitative luciferase comparison was based on fluorescence measurements before the transplantation to ensure equal expression ratios of imaging reporter. The remaining fluctuation between different animals for one luciferase is most probably due to the not avoidable error induced by the transplantation procedure. Nevertheless, the quantitative analysis demonstrates robustly that Luc2 is the best choice for single reporter neuroimaging.

One reason for this effect was elucidated by the analysis of emission spectra. At deep locations in the brain, attenuation of bioluminescence transmission by light absorption owing to hemoglobin (42,43) and light scattering at myelin/cell boarders (44) becomes more pronounced. Therefore, the relation between Luc2 and PpyRE9 decreased (from 4.5 ± 0.2 to 3.7 ± 0.3) under in *in vivo* conditions. In case of a more red-shifted luciferase (e.g. emission peak > 620 nm) this spectral benefit could gain more importance and even change the order of the best luciferase. We detected a significant difference between CBG99 and Luc2 in line with the *in vitro* results. Interestingly, the green luciferase CBG99 spectrum was modulated in a transplantation depth-dependent manner. The CBG99 spectrum is predominantly attenuated in the green spectral region, the most prominent region for hemoglobin absorption (530–580 nm) (41). The attenuation of the green part of the CBG99 spectrum is directly related to changes described by Zhao and colleagues (41) for CBG68, but even more pronounced in the brain. The shift in emission maximum could serve as a noninvasive estimation for the cell graft location, for example in longitudinal studies in which migration of stem cells may take place from the implantation site to deeper (or more superficial) brain areas. In this case, spectral recording of the CBG99 signal would resolve the emission maximum, which could be translated to a certain transplantation depth (cf. Supporting Information, Fig. S3).

The analysis of the Coelenterazine h-dependent hRluc revealed no change in the spectrum compared with *in vitro* conditions, but a faster kinetic *in vivo* and the smallest photon flux compared with the D-luciferin-dependent luciferases. The small photon emission could be reversed by i.v. injections. However, we found this injection route not applicable for repetitive *in vivo* measurements because of the toxicity of Coelenterazine h (it can lead to necrosis; the lethal dose was reached already at 2× the standard dose). By following the hRluc BLI signal for one week, we detected a very high signal only shortly after the transplantation, which was most likely due to the disturbed blood–brain barrier after surgery. As a third limitation of Coelenterazine h-based imaging, it has been repored that

Coelenterazine is actively transported out of the brain parenchyma via the multidrug resistance MDR1 P-glycoprotein (18,19). Based on our i.p. and i.v. comparison, the emission spectrum and the strong signal decrease over time, we conclude that hRluc *in vivo* neuroimaging is highly limited by a combination of restricted substrate availability, fast kinetics and light emission in the blue range. We could not detect hRluc expressed by NSCs, which is directly related to the 5-fold difference in gene expression compared with the HEK-293 cells. However, NSC tracking with hRluc should be feasible, for example, by increasing the number of injected NSCs or novel methods to increase the reporter gene expression while retaining stem cell properties.

4.3. Validation of Dual Reporter Neuroimaging

We explored the possibility of dual reporter imaging in the brain using the HEK-293 cells, owing to their superior reporter expression levels. The Luc2/hRluc luciferases were separated well in the mixed HEK-293 cell graft. The substrate specificity, recently proven by Bhaumik and colleagues (31) to have no crossreactivity between D-luciferin and Coelenterazine, is one clear advantage for using these luciferases to elucidate different processes in one animal. In contrast to dual reporter imaging with subcutaneous or lung transplants enabling higher photon fluxes from hRluc (45) our approach for brain imaging clearly revealed a much stronger Luc2 signal. This is in accordance with the luciferase comparison data from separated cell grafts.

We discriminated transplanted NSC populations with D-luciferin-dependent luciferases based on the different emission spectra in separate experiments. The luciferases CBG99 and PpyRE9 were chosen in reference to our previous achievements of dual color imaging in the superficial tissues prostate and liver (8). However, the brain application revealed strong limitations for combining the green CBG99 and the red PpyRE9 for sensitive dual color imaging. In particular, the strong attenuation of the green part of the CBG99 emission spectrum lead to a substantial spectral overlay with PpyRE9 and allowed only qualitative spectral unmixing. As discussed above, the dual color approach in the brain would benefit from firefly mutants with even higher photon emission in the red and far-red range.

5. CONCLUSION

This quantitative comparison of Luc2, PpyRE9, CBG99 and hRluc for tracking of NSC in the mouse brain provides detailed characterization of bioluminescence kinetics, spectra of emission and sensitivity. The results underline the superiority of Luc2 in terms of sensitivity in deep brain tissue. The luciferases were expressed in two cell types (HEK-293 and NSCs) revealing cell type-specific transgene expression. The proof-of-principle dual reporter neuroimaging experiments (Luc2/hRluc and CBG99/PpyRE) underline the potential, but also the challenges for a cell tracking approach with two distinct optical readouts.

Acknowledgments

We gratefully acknowledge Gabriele Schneider, Nadine Henn, Ivo Que and Martijn Rabelink for excellent technical support and Eric Kaijzel for valuable comments and helpful discussions. This work was supported by the funds from the EU-FP7 programs ENCITE (HEALTH-F5-2008-201842) and TargetBraIn (HEALTH-F2-2012-279017) and by a fund from the Volkswagen Foundation (I/83 443).

6. CONFLICT OF INTEREST

The authors declare that they have no conflicts of interest.

REFERENCES

1. Edinger M, Sweeney TJ, Tucker AA, Olomu AB, Negrin RS, Contag CH. Noninvasive assessment of tumor cell proliferation in animal models. Neoplasia 1999; 1(4): 303–310.
2. Kim DE, Schellingerhout D, Ishii K, Shah K, Weissleder R. Imaging of stem cell recruitment to ischemic infarcts in a murine model. Stroke 2004; 35(4): 952–957.
3. Kadurugamuwa JL, Francis KP. Bioluminescent imaging of bacterial biofilm infections in vivo. Meth Mol Biol 2008; 431: 225–239.
4. Chewning JH, Dugger KJ, Chaudhuri TR, Zinn KR, Weaver CT. Bioluminescence-based visualization of CD4 T cell dynamics using a T lineage-specific luciferase transgenic model. BMC Immunol 2009; 10: 44.
5. de Almeida PE, van Rappard JRM, Wu JC. In vivo bioluminescence for tracking cell fate and function. Am J Physiol Heart Circul Physiol 2011; 301(3): H663–H671.
6. Deroose CM, Reumers V, Gijsbers R, Bormans G, Debyser Z, Mortelmans L, Baekelandt V. Noninvasive monitoring of long-term lentiviral vector-mediated gene expression in rodent brain with bioluminescence imaging. Mol Ther 2006; 14(3): 423–431.
7. Shah K, Weissleder R. Molecular optical imaging: applications leading to the development of present day therapeutics. NeuroRx 2005; 2(2): 215–225.
8. Mezzanotte L, Que I, Kaijzel E, Branchini B, Roda A, Lowik C. Sensitive dual color in vivo bioluminescence imaging using a new red codon optimized firefly luciferase and a green click beetle luciferase. PLoS One 2011; 6(4): e19277.
9. Nakatsu T, Ichiyama S, Hiratake J, Saldanha A, Kobashi N, Sakata K, Kato H. Structural basis for the spectral difference in luciferase bioluminescence. Nature 2006; 440(7082): 372–376.
10. Michelini E, Cevenini L, Mezzanotte L, Ablamsky D, Southworth T, Branchini B, Roda A. Spectral-resolved gene technology for multiplexed bioluminescence and high-content screening. Anal Chem 2008; 80(1): 260–267.
11. Branchini BR, Ablamsky DM, Davis AL, Southworth TL, Butler B, Fan F, Jathoul AP, Pule MA. Red-emitting luciferases for bioluminescence reporter and imaging applications. Anal Biochem 2010; 396(2): 290–297.
12. Wood KV, Lam YA, Seliger HH, McElroy WD. Complementary DNA coding click beetle luciferases can elicit bioluminescence of different colors. Science 1989; 244(4905): 700–702.
13. Tannous BA. Gaussia luciferase reporter assay for monitoring biological processes in culture and in vivo. Nat Protocols 2009; 4(4): 582–591.
14. Verhaegen M, Christopoulos TK. Recombinant Gaussia luciferase. Overexpression, purification, and analytical application of a bioluminescent reporter for DNA hybridization. Anal Chem 2002; 74(17): 4378–4385.
15. Matthews JC, Hori K, Cormier MJ. Purification and properties of Renilla reniformis luciferase. Biochemistry 1977; 16(1): 85–91.
16. Nakajima Y, Kobayashi K, Yamagishi K, Enomoto T, Ohmiya Y. cDNA cloning and characterization of a secreted luciferase from the luminous Japanese ostracod, Cypridina noctiluca. Biosci Biotechnol Biochem 2004; 68(3): 565–570.
17. Baldwin TO, Berends T, Bunch TA, Holzman TF, Rausch SK, Shamansky L, Treat ML, Ziegler MM. Cloning of the luciferase structural genes from Vibrio harveyi and expression of bioluminescence in Escherichia coli. Biochemistry 1984; 23(16): 3663–3667.
18. Close DM, Patterson SS, Ripp S, Baek SJ, Sanseverino J, Sayler GS. Autonomous bioluminescent expression of the bacterial luciferase gene cassette (lux) in a mammalian cell line. PLoS One 2010; 5(8).
19. Reumers V, Deroose CM, Krylyshkina O, Nuyts J, Geraerts M, Mortelmans L, Gijsbers R, Van den Haute C, Debyser Z, Baekelandt V. Noninvasive and quantitative monitoring of adult neuronal stem cell migration in mouse brain using bioluminescence imaging. Stem Cells 2008; 26(9): 2382–2390.

20. Geraerts M, Eggermont K, Hernandez-Acosta P, Garcia-Verdugo JM, Baekelandt V, Debyser Z. Lentiviral vectors mediate efficient and stable gene transfer in adult neural stem cells in vivo. Hum Gene Ther 2006; 17(6): 635–650.
21. Sher F, van Dam G, Boddeke E, Copray S. Bioluminescence imaging of Olig2-neural stem cells reveals improved engraftment in a demyelination mouse model. Stem Cells 2009; 27(7): 1582–1591.
22. Liang Y, Walczak P, Bulte JW. Comparison of red-shifted firefly luciferase Ppy RE9 and conventional Luc2 as bioluminescence imaging reporter genes for in vivo imaging of stem cells. J Biomed Opt 2012; 17(1): 016004.
23. Ibrahimi A, Vande Velde G, Reumers V, Toelen J, Thiry I, Vandeputte C, Vets S, Deroose C, Bormans G, Baekelandt V, Debyser Z, Gijsbers R. Highly efficient multicistronic lentiviral vectors with peptide 2A sequences. Hum Gene Ther 2009; 20(8): 845–860.
24. Conti L, Pollard SM, Gorba T, Reitano E, Toselli M, Biella G, Sun YR, Sanzone S, Ying QL, Cattaneo E, Smith A. Niche-independent symmetrical self-renewal of a mammalian tissue stem cell. PLoS Biol 2005; 3(9): 1594–1606.
25. Wray JP. Characterisation of a novel culture condition for the establishment and maintenance of mouse embryonic stem cells and implications for the mechanisms of self-renewal. PhD thesis University of Edinburgh, 2009.
26. Doetschman TC, Eistetter H, Katz M, Schmidt W, Kemler R. The in vitro development of blastocyst-derived embryonic stem cell lines: formation of visceral yolk sac, blood islands and myocardium. J Embryol Exp Morphol 1985; 87: 27.
27. Pfannkuche K, Liang HM, Hannes T, Xi JY, Fatima A, Nguemo F, Matzkies M, Wernig M, Jaenisch R, Pillekamp F, Halbach M, Schunkert H, Saric T, Hescheler J, Reppel M. Cardiac myocytes derived from murine reprogrammed fibroblasts: intact hormonal regulation, cardiac ion channel expression and development of contractility. Cell Physiol Biochem 2009; 24(1–2): 73–86.
28. Aswendt M. Imaging beyond structure – novel noninvasive tools for neuroimaging of stem cell function and differentiation. Otto von Guericke University: Magdeburg, 2013.
29. Carlotti F, Bazuine M, Kekarainen T, Seppen J, Pognonec P, Maassen JA, Hoeben RC. Lentiviral vectors efficiently transduce quiescent mature 3 T3-L1 adipocytes. Mol Ther 2004; 9(2): 209–217.
30. Gil JS, Machado HB, Herschman HR. A method to rapidly and accurately compare the relative efficacies of non-invasive imaging reporter genes in a mouse model and its application to luciferase reporters. Mol Imag Biol 2012; 14(4): 462–471.
31. Bhaumik S, Gambhir SS. Optical imaging of Renilla luciferase reporter gene expression in living mice. Proc Natl Acad Sci USA 2002; 99(1): 377–382.
32. Ignowski JM, Schaffer DV. Kinetic analysis and modeling of firefly luciferase as a quantitative reporter gene in live mammalian cells. Biotechnol Bioeng 2004; 86(7): 827–834.
33. Gassmann M, Donoho G, Berg P. Maintenance of an extrachromosomal plasmid vector in mouse embryonic stem cells. Proc Natl Acad Sci USA 1995; 92(5): 1292–1296.
34. Camenisch G, Gruber M, Donoho G, Van Sloun P, Wenger RH, Gassmann M. A polyoma-based episomal vector efficiently expresses exogenous genes in mouse embryonic stem cells. Nucl Acids Res 1996; 24(19): 3707–3713.
35. Dhara SK, Gerwe BA, Majumder A, Dodla MC, Boyd NL, Machacek DW, Hasneen K, Stice SL. Genetic manipulation of neural progenitors derived from human embryonic stem cells. Tissue Eng Part A 2009; 15(11): 3621–3634.
36. Okada S, Ishii K, Yamane J, Iwanami A, Ikegami T, Katoh H, Iwamoto Y, Nakamura M, Miyoshi H, Okano HJ, Contag CH, Toyama Y, Okano H. In vivo imaging of engrafted neural stem cells: its application in evaluating the optimal timing of transplantation for spinal cord injury. FASEB J 2005; 19(13): 1839–1841.
37. Puttonen KA, Ruponen M, Kauppinen R, Wojciechowski S, Hovatta O, Koistinaho J. Improved method of producing human neural progenitor cells of high purity and in large quantities from pluripotent stem cells for transplantation studies. Cell Transplantation 2012. DOI:10.3727/096368912X658764
38. Wu JC, Cao F, Dutta S, Xie XY, Kim E, Chungfat N, Gambhir S, Mathewson S, Connolly AJ, Brown M, Wang EW. Proteomic analysis of reporter genes for molecular imaging of transplanted embryonic stem cells. Proteomics 2006; 6(23): 6234–6249.
39. Mezzanotte L, Fazzina R, Michelini E, Tonelli R, Pession A, Branchini B, Roda A. In vivo bioluminescence imaging of murine xenograft cancer models with a red-shifted thermostable luciferase. Mol Imag Biol 2010; 12(4): 406–414.
40. Miloud T, Henrich C, Hammerling GJ. Quantitative comparison of click beetle and firefly luciferases for in vivo bioluminescence imaging. J Biomed Opt 2007;12(5): 054018.
41. Zhao H, Doyle TC, Coquoz O, Kalish F, Rice BW, Contag CH. Emission spectra of bioluminescent reporters and interaction with mammalian tissue determine the sensitivity of detection in vivo. J Biomed Opt 2005;10(4): 41210.
42. Tuchin VV. Tissue Optics: Light Scattering Methods and Instruments for Medical Diagnosis, Vol. XXV. SPIE Press: Bellingham, WA, 2000; 352.
43. Van der Zee P. Measurement and Modelling of the Optical Properties of Human Tissue in the Near Infrared. University of London: London, 1992.
44. Ross KFA. Phase Contrast and Interference Microscopy for Cell Biologists, Vol. XXI. Edward Arnold: London, 1967; 238.
45. Bhaumik S, Lewis XZ, Gambhir SS. Optical imaging of Renilla luciferase, synthetic Renilla luciferase, and firefly luciferase reporter gene expression in living mice. J Biomed Opt 2004; 9(3): 578–586.
46. Branchini BR, Ablamsky DM, Murtiashaw MH, Uzasci L, Fraga H, Southworth TL. Thermostable red and green light-producing firefly luciferase mutants for bioluminescent reporter applications. Anal Biochem 2007; 361(2): 253–262.

SUPPORTING INFORMATION

Supporting information can be found in the online version of this article.

